Ab initio study of an iron atom interacting with single-wall carbon nanotubes

Solange B. Fagan and R. Mota
Departamento de Física, Universidade Federal de Santa Maria, CEP 97105-900 Santa Maria, RS, Brazil

Antônio J. R. da Silva and A. Fazzio
Instituto de Física, Universidade de São Paulo, Caixa Postal 66318, CEP 05315-970 São Paulo, SP, Brazil
(Received 11 September 2002; revised manuscript received 6 February 2003; published 20 May 2003)

The interaction of an iron atom with a single-wall carbon nanotube is investigated using spin-polarized total-energy first-principles calculations. A systematic study for the atom approaching the tube surface, both from outside and inside, is presented for several configurations to determine the equilibrium distances and the binding energies. It is shown that when the atom interacts with the tube from outside, a $3d^7\ 4s^1$ effective configuration is obtained and the total magnetization is close to the atomic value. For the inside case, as a consequence of higher hybridization and a confinement effect, the magnetization decreases and the finally obtained effective configuration is $3d^8\ 4s^0$.

DOI: 10.1103/PhysRevB.67.205414 PACS number(s): 73.61.Wp, 72.80.Rj, 71.15.Nc

I. INTRODUCTION

The high potential of carbon nanotubes for fundamental studies and technical applications is due to their peculiar physical, chemical, and mechanical properties.[1,2] Consequently, they are candidates to constitute building blocks for nanoelectronic devices by themselves, and also through the combination with other elements. One of the proposed routes towards new materials with specific properties has been to associate single-wall carbon nanotube (SWCN) with transition-metals (TM) atoms.

The physical properties of TM atoms adsorbed on SWCN are certainly of great current interest in nanophysics. Recently, a few theoretical[3] and experimental[4] works related to TM interacting with SWCN have been reported in the literature. Nevertheless, a complete understanding of the interaction between TM atoms and SWCN remains a challenging issue. For instance, SWCN is synthesized using a combination of catalyst TM particles and dense carbon vapor.[5] The exact growth mechanism of SWCN during the closer encounter of carbon vapor with TM atoms is not completely clear and the key role played by TM atoms in the production of SWCN is still under investigation.

The reduction of the contact resistance between nanotubes and TM atoms, which is a critical problem in the nanoelectronic applications, specially those based on spintronic, requires a better understanding of the interaction between them. The bonding of the atoms on SWCN has been shown to depend on the detailed contact conditions.[6,7] Moreover, there is an extraordinary interest about the magnetic order in low-dimensional systems. SWCN covered with TM atoms presenting magnetic order provides an unique interesting field to discuss magnetic behavior at surfaces with quasi-one-dimensional character. In particular, encapsulating ferromagnetic structures inside carbon nanotubes has become an active research topic for their potential applications in recording media and magnetic inks.[8]

In contrast to the lack of detailed studies of TM atoms interacting with SWCN, the interactions of these atoms with graphite have been extensively investigated, both experimentally[9] and theoretically.[10] Different from graphite or graphene, SWCN makes the problem much more exciting, since the tube curved surface (i) does not present a pure sp^2 hybridization, with a resulting mixing between σ and π states, and (ii) leads to the confinement of states around the tube circumference, and therefore, we should expect a different behavior for TM atoms on SWCN when compared with graphite sheet.[11]

The first step towards the understanding of all the problems pointed out above is the complete understanding of the structural, electronic, and magnetic properties of a single TM atom interacting with an SWCN. In this work, a systematic study of an iron atom adsorbed on SWCN through spin-polarized total-energy first-principles calculations is performed. In the following section we present the method used in all our calculations, followed by a discussion of our results and the overall conclusions.

II. CALCULATIONS PROCEDURE

Our study is based on first-principles spin-polarized density-functional theory.[12] We have used the SIESTA code,[13] which performs fully self-consistent calculation solving the standard Kohn-Sham (KS) equations. The KS orbitals are expanded using linear combinations of pseudoatomic orbitals proposed by Sankey and Niklewski.[14] In all calculations, we have used a double-zeta basis set with polarization functions.[15] For the exchange and correlation term, the generalized gradient approximation (GGA) is used as proposed by Perdew-Burke-Ernzerhof.[16] The standard norm conserving the Troullier-Martins pseudopotential is adopted.[17] A cutoff of 150 Ry for the grid integration was utilized to represent the charge density. We have used 15 Monkhorst-Pack k points for the Brillouin-zone integration along the tube axis. The relaxed atomic configurations of the tubes were obtained by a minimization of the total energy using the Hellman-Feymann forces including Pulay-like corrections. Structural optimizations were performed using the conjugate gradient algorithm until the residual forces were smaller than 0.05 eV/Å.

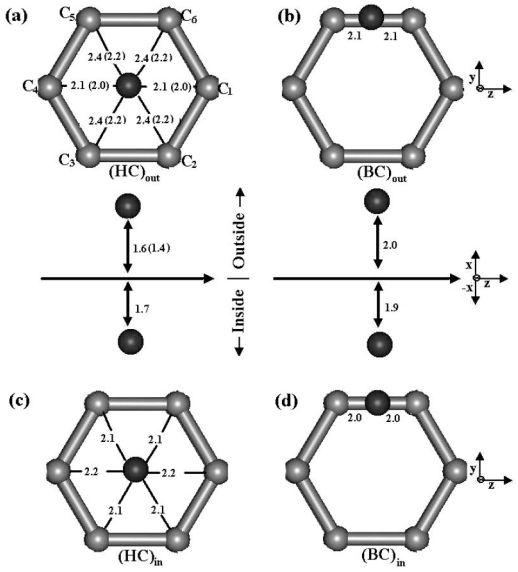

FIG. 1. Final full-relaxed structural configurations for the Fe-tube configurations (a) $(HC)_{out}$, (b) $(BC)_{out}$, (c) $(HC)_{in}$, and (d) $(BC)_{in}$.

The adopted SWCN is the zigzag (8,0), which is known to be a semiconductor. For the pure tube, we obtain a gap of 0.55 eV and a diameter of 6.26 Å. We use periodic-boundary conditions and a supercell approximation, with 64 C atoms plus one Fe atom, with a resulting length of 8.52 Å. This should be enough to make sure that the Fe atoms in neighboring cells do not interact with each other. We use a lateral separation of 15 Å between tube centers, which prevents any tube-tube interaction.

III. RESULTS AND DISCUSSION

Six distinct sites are considered to investigate the interaction of a single Fe atom adsorbed on the (8,0) SWCN surface. These initial sites are described in the following way: three from inside (subscript in); one with the atom approaching the center of a hexagon $(HC)_{in}$; one with the atom along a direction perpendicular to the tube surface and pointing towards the middle of C-C bond $(BC)_{in}$; and one directly above a C atom $(TOP)_{in}$; three similar configurations with the Fe atom outside the nanotube (subscript out), labeled $(HC)_{out}$, $(BC)_{out}$, and $(TOP)_{out}$, respectively. All sites have been studied in such a way that the energies were minimized and all the atoms were allowed to relax.

The final fully relaxed structural configurations are shown in Fig. 1 for the four most stable ones: (a) $(HC)_{out}$, (b) $(BC)_{out}$, (c) $(HC)_{in}$, and (d) $(BC)_{in}$. For the (HC) configurations, the initially assumed positions were symmetrical with respect to the carbon hexagonal atoms; after the optimization, as seen in Fig. 1(a), the resulting asymmetry is noticeable. There are two sets of similar bonds between the Fe and C atoms, one with four (to the atoms C_2, C_3, C_5, and C_6) and the other with two (to the atoms C_1 and C_4) bonds, which is related to a mirror plane parallel to the tube axis and that passes through the (HC) site and the C_1 and C_4 atoms. Whereas in $(HC)_{out}$ the approaching atom gets closer to C_1 and C_4, when compared to the distances to the other four C atoms, the opposite is true for $(HC)_{in}$. This can be understood as a consequence of the tube curvature. From inside there is a concave geometry whereas from outside the Fe atom approaches a convex geometry. The equilibrium distances from the center of the hexagon, characterizing the tube surface, to the Fe atom are 1.6 Å for $(HC)_{out}$ and 1.7 Å for $(HC)_{in}$. The similar equilibrium distances for the (BC) configurations are bigger than the corresponding (HC). As shown in Figs. 1(b) and 1(d), they are 2.0 Å and 1.9 Å for $(BC)_{out}$ and $(BC)_{in}$, respectively. This occurs in order that the Fe-C bond lengths can become $\simeq 2.$ Å.

TABLE I. Binding energies (E_b) for all the Fe configurations. The total magnetization M, as well as its contributions from $4s$ (m_s), $4p$ (m_p), and $3d$ (m_d) orbitals are shown.

Fe-position	E_b(eV)	M(μ_B)	$m_s(\mu_B)$	$m_p(\mu_B)$	$m_d(\mu_B)$
$(HC)_{out}$	−1.40	3.90	0.48	0.25	3.07
$(BC)_{out}$	−0.85	3.92	0.61	0.21	3.21
$(TOP)_{out}$	−0.65	3.93	0.60	0.20	3.14
$(HC)_{in}$	−1.07	2.36	0.02	0.07	2.38
$(BC)_{in}$	−1.15	2.22	0.02	0.06	2.29
$(TOP)_{in}$	−0.80	2.44	0.04	0.04	2.46

In Fig. 1(a), the numbers in parenthesis are those obtained through calculations not including spin polarization. Note that, even for structural properties, the inclusion or not of spin polarization leads to different results; if spin polarization is not taken into account, the equilibrium distances are around 0.2 Å shorter.

The calculated binding energies for all studied sites are summarized in Table I. The binding energies are calculated through the expression

$$E_b = E_{(tube+Fe)} - E_{(tube)} - E_{(Fe)}, \tag{1}$$

where $E_{(tube+Fe)}$ is the spin-polarized total energy for the equilibrium structure of the (8,0) tube plus the adsorbed Fe atom, $E_{(tube)}$ is the energy of the isolated tube, and $E_{(Fe)}$ is the spin-polarized total energy of an Fe atom at the $3d^6 4s^2$ ground-state configuration. We obtain as the most stable configuration the $(HC)_{out}$ site, as can be seen in Table I. Except for the (HC) site, the ''in'' positions have lower binding energies than the corresponding ''out'' positions. These differences, however, will tend to zero as the diameter of the nanotube increases.

In Figs. 2 and 3 the band structures are shown for the $(HC)_{out}$ and $(HC)_{in}$ configurations, respectively. In the left side of these figures it is presented, for comparison, the band structure for the isolated (8,0) tube. The bands are seen separately for up (majority) and down (minority) spins. In Fig. 2(b), a level with predominant 4s character from the Fe atom appears in the gap region, with a rather small dispersion. This very flat level is a consequence of the small interaction between the iron atoms in different cells, either directly or through the nanotubes states. The majority spin bands with predominant Fe d character appear resonant in the SWCN valence band, being located approximately between 2.0 eV

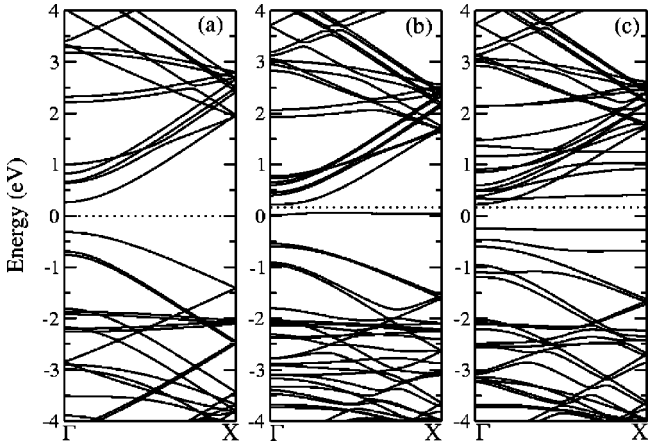

FIG. 2. Band structures for (a) the pure SWCN (8,0); (b) the $(HC)_{out}$ majority spins; and (c) the $(HC)_{out}$ minority spins. The dashed lines correspond to the Fermi energy.

and 3.0 eV bellow the top of the valence band. In the case of minority spins [Fig. 2(c)] the Fe atom introduces a very localized state with *d* character in the energy gap. There is also one *d*-character resonant state that interacts with the top of valence band, leading to the splitting of the originally twice degenerated level. The other down orbitals with *d* character are located inside the conduction band. The band structure for the Fe atom located at $(HC)_{out}$ indicates that there is a charge transfer from the Fe 4*s* orbital to the Fe 3*d* orbital, leading to an effective $3d^7 4s^1$ atomic configuration. The overall characteristics of the $(BC)_{out}$ and $(TOP)_{out}$ band structures are very similar to these ones, making it redundant to discuss those results here.

In Fig. 3 we show the band structure for Fe in the $(HC)_{in}$ site. Even though the local symmetry is similar (an Fe atom surrounded by 6 C atoms), the fact that the Fe is now inside the tube changes its electronic structure in a significant way. For example, it can be seen from Fig. 3(b) for the majority spins band structure that the 4s orbital that appeared in the energy gap for $(HC)_{out}$ is now absent, being higher up in energy. This could be a result of a confinement effect, and as

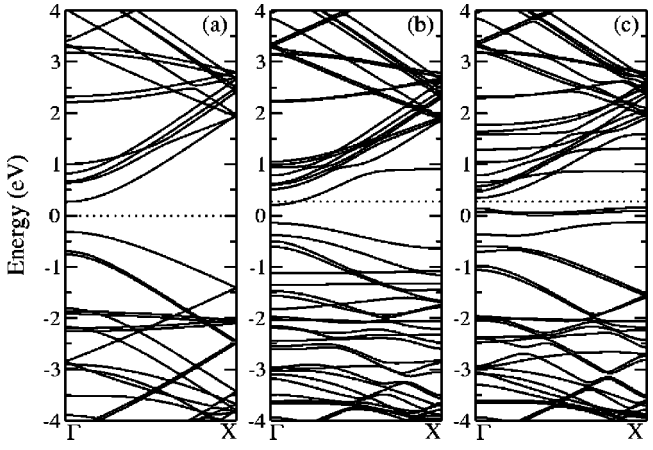

FIG. 3. Band structures for (a) the pure SWCN (8,0); (b) the $(HC)_{in}$ majority spins; and (c) the $(HC)_{in}$ minority spins. The dashed lines correspond to the Fermi energy.

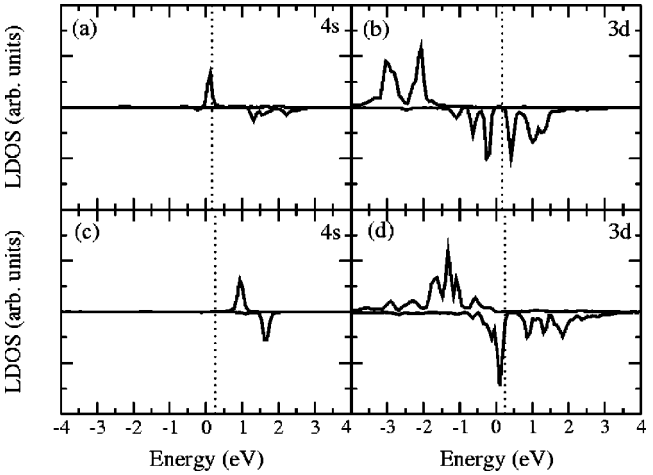

FIG. 4. The local density of states projected onto the Fe atom for $l=0$ and $l=2$. (a) $(HC)_{out} l=0$; (b) $(HC)_{out} l=2$; (c) $(HC)_{in} l=0$; and (d) $(HC)_{in} l=2$. The dashed lines correspond to the Fermi energy.

such may disappear as the tube diameter increases. From the figure we can also observe the strong change in the bottom of conduction band due to the strong interaction between the 4*s*-up orbitals and the π^* states. Moreover, the valence bands are strongly modified due to the coupling to the 3*d* Fe orbitals. In conclusion, for $(HC)_{in}$, the occupied states have very little contribution from the 4*s* orbitals and have a stronger hybridization between the tube states and the Fe-*d* orbitals, when compared to $(HC)_{out}$. In the minority spins bands [Fig. 3(c)], the three occupied states, with small dispersions in the gap, have a strong Fe-*d* character. Therefore, when the Fe ion is inside the tube there is a substantial charge transfer between the 4*s* and 3*d* Fe orbitals, resulting in an effective $d^8 s^0$ configuration for the Fe, similarly to interstitial Fe in semiconductors.[18]

To have a better understanding of the role played by Fe in the nanotube, we present in Fig. 4 the projected local density of states onto the Fe-atom, for $l=0$ and $l=2$. Analyzing the $l=0$ (4*s*), it is clear that for $(HC)_{in}$ [Fig. 4(c)], there is no contribution from the 4*s* orbital to the occupied states, since almost all the 4*s* weight is located above the Fermi energy. In contrast, for the $(HC)_{out}$ an occupied 4*s*-state is observed very close to the bottom of the conduction band, as seen in Fig. 4(a). For the inside Fe, the 3*d* orbitals [Fig. 4(d)] present higher dispersions and are energetically closer to the top of the valence band when compared to the outside case [Fig. 4(b)]. For the outside Fe there is a transfer of one electron from the 4*s* orbital to the 3*d* orbital, which is related to a decrease of the intra-*d* Coulomb repulsion. For the Fe inside case, not only there is this Coulomb repulsion decreasing, but there is also a confinement of the *s* states, which results in the transfer of two electrons to the *d* orbitals. In conclusion, we can say that a free Fe atom $(3d^6 4s^2)$, when interacting with an SWCN from outside, will have an effective $3d^7 4s^1$ configuration, whereas, when it interacts with the nanotube from inside (for small tube diameters), an effective $3d^8 4s^0$ configuration will result. Assuming the same behavior for the other transition metals, one would expect

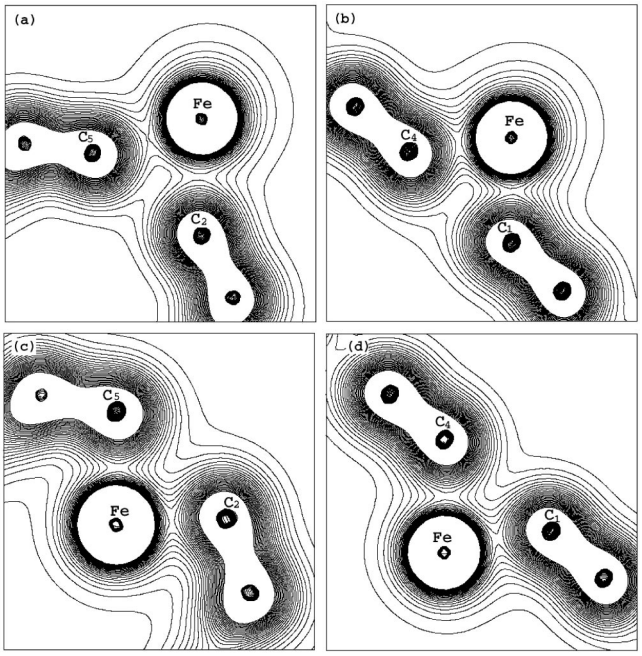

FIG. 5. Contour plots of the total charge density for both the $(HC)_{out}$ and the $(HC)_{in}$ configurations. For $(HC)_{out}$, we show the results for (a) a plane that passes through the C_5-Fe-C_2 atoms and (b) a plane that passes through the C_4-Fe-C_1 atoms. For $(HC)_{in}$, we present the results for (c) a plane that passes through the C_5-Fe-C_2 atoms and (d) a plane that passes through the C_4-Fe-C_1 atoms. The labeled C atoms are shown in Fig. 1. The outermost and the innermost contour lines correspond to 0.003 e/Å^3 and 0.099 e/Å^3, respectively, and the contour line spacing is 0.004 e/Å^3.

that an Ni atom inside the nanotube would have an effective $3d^{10}4s^0$. This would probably lead to a situation where the Ni atom would have a very weak interaction with the SWCN, a behavior already seen by Andriotis *et al.*[3]

The ratio Δ_{ex}/Δ_{CF} between the exchange splitting (Δ_{ex}) and the crystal-field splitting (Δ_{CF}) gives us information about the localization of the d orbitals. A typical highly localized state with a strong atomic character occurs for $\Delta_{ex}/\Delta_{CF} \gg 1$. In our case, we estimate[19] Δ_{ex}/Δ_{CF} around 4.5 for Fe in $(HC)_{out}$ and 3.0 for $(HC)_{in}$. These values indicate a non-negligible hybridization between the Fe-ions and the tube. The effect of this hybridization can be clearly seen in Fig. 5, where we present contour plots of the total charge density for both the $(HC)_{out}$ and the $(HC)_{in}$ configurations. As can be seen in this figure, there is a clear covalent character in the interaction between the Fe atom and the SWCN, for the outside as well as for the inside configurations. In Fig. 5(a), we show the contour plot for the $(HC)_{out}$ case in a plane that passes through the C_5-Fe-C_2 atoms, whereas in Fig. 5(b), we present a similar plot [also for $(HC)_{out}$] in a plane that passes through the C_4-Fe-C_1 atoms. As can be seen, the interaction is stronger (characterized by a larger value of the charge density between the Fe-C atoms) for this latter situation, which is consistent with the smaller values of the Fe-C_4 and the Fe-C_1 bond lengths when compared to the Fe-C_5 and the Fe-C_2 bond lengths. On the other hand, for the $(HC)_{in}$ we obtain the opposite behavior, with a stronger interaction between the Fe-C_5 and the Fe-C_2 bonds than between the Fe-C_4 and the Fe-C_1 bonds, as can be seen in Figs. 1(c) and 1(d). This happens because for the inside configuration, as opposed to the Fe outside structure, the bond lengths for the Fe-C_5 and Fe-C_2 bonds are the smaller ones. Therefore, the large observed values for the binding energies have a clear covalent-bond character contribution. Moreover, a binding energy value of the order of 2 eV is also observed for the interaction of Fe with graphite[10] and with the benzene molecule.[20]

We also examine the magnetic moments that are shown in Table I. The total magnetic moments *M* for the Fe in the outside configurations are higher than inside configurations, as a consequence of both a smaller hybridization for the outside as well as an *s*-orbital confinement for the inside structures. In general, except for the $(TOP)_{out}$ configuration, the tube presents a net antiparallel magnetization when compared to the Fe-ion magnetization, of the order of $0.1\mu_B$. It is interesting to compare our results with the results for Fe on graphite[10] and Fe on benzene.[20] The Fe magnetic moment for both the graphite as well as the benzene case has been obtained[10,20] to have a value of $2\mu_B$. This should be contrasted to the larger values obtained in the present case of $3.9\mu_B$ for the $(HC)_{out}$ configuration and $2.4\mu_B$ for the $(HC)_{in}$ configuration. To understand this different behavior, we have also performed a calculation for Fe on benzene. Similar to what has been obtained by Pandey *et al.*,[20] we have also obtained in this case an Fe magnetic moment of approximately $2\mu_B$. However, to study the effect of the curvature on the Fe magnetic moment, we raised two diametrically opposite C atoms of the benzene molecule outside of the molecular plane, and considered two situations, one where the Fe atom is closer to these two atoms and further away from the four remaining C atoms, and another where the Fe atom is closer to the four remaining C atoms than to the two raised C atoms. This latter situation is similar to the $(HC)_{in}$ configuration, whereas the former one is similar to the $(HC)_{out}$ configuration. In both the cases we obtain an increase in the Fe magnetic moment to a value close to $4\mu_B$, similar to what we obtain for the Fe in the $(HC)_{out}$ configuration (not only the total magnetic moment is similar, but also the individual *s*, *p*, and *d* contributions). This indicates that the effect of curvature is responsible for the increase in the Fe magnetic moment from $2\mu_B$ to $4\mu_B$. However, for the $(HC)_{in}$ configuration we do not observe such high value for the Fe magnetic moment. This is caused by the confinement effect mentioned previously, which leads to an electron transfer from the Fe *s* orbital to the Fe *d* orbitals.

IV. CONCLUSIONS

In conclusion, this paper presents a systematic understanding of the structural, electronic, and magnetic properties of a single Fe atom interacting with a (8,0) SWCN. The final fully relaxed structural configurations and the equilibrium distances from the tube surface to the Fe atom, approaching from outside and inside, were determined for different positions. The most stable configuration is determined to be $(HC)_{out}$, similar to what is found for the adsorption of Fe in

graphite.[10] Moreover, the energy difference between the $(HC)_{out}$ and $(TOP)_{out}$ configurations is also similar to what is found for Fe in graphite.[10] The importance of taking into account the spin polarization in the calculations was emphasized, even for structural properties. In terms of electronic structure, it was demonstrated that when the Fe atom interacts with an SWCN from outside an effective $3d^7 4s^1$ configuration results as a consequence of a decreasing in the intra-*d* Coulomb repulsion and a curvature effect. For the Fe inside cases, there is also a confinement of the *s* states, which results in a complete migration of the two electrons to the *d*-orbitals, leading to a $3d^8 4s^0$ final effective configuration. The smaller hybridization for the outside compared with the inside cases, as with well as confinement states for the inside positions, help to elucidate the higher total magnetic moments observed in the outside configurations.

[1] H. Dai, Surf. Sci. **500**, 218 (2002).

[2] M.S. Dresselhaus, G. Dresselhaus, and P. Avouris, *Carbon Nanotubes* (Springer, Berlin, 2001).

[3] A.N. Andriotis, M. Menon, and G. Froudakis, Phys. Rev. Lett. **85**, 3193 (2000); A.N. Andriotis, M. Menon, and G. Froudakis, Phys. Rev. B **61**, R13 393 (2000); A.N. Andriotis, M. Menon, and G. Froudakis, Chem. Phys. Lett. **320**, 425 (2000); Y.H. Lee, S.G. Kim, and D. Tomanek, Phys. Rev. Lett. **78**, 2393 (1997); K. Kong, S. Han, and J. Ihm, Phys. Rev. B **60**, 6074 (1999).

[4] Y. Zhang, N.W. Franklin, R.J. Chen, and H. Dai, Chem. Phys. Lett. **331**, 35 (2000).

[5] C. Journet, W. Maser, P. Bernier, A. Loiseau, M. Delachapelle, S. Lefrant, P. Deniard, R. Lee, and J. Fischer, Nature (London) **388**, 756 (1997); G.G. Tibbetts, M.G. Devour, and E.J. Rodda, Carbon **25**, 367 (1987).

[6] A.N. Andriotis, M. Menon, and G. Froudakis, Appl. Phys. Lett. **76**, 3890 (2000).

[7] K. Tsukagoshi, B. Alphenaar, and H. Ago, Nature (London) **401**, 572 (1999); M.B. Nardelli, J.L. Fattebert, and J. Bernholc, Phys. Rev. B **64**, 245423 (2001).

[8] A.A. Setlur, J.Y. Dai, J.M. Lauerhaas, P.L. Washington, and R.P.H. Chang, J. Mater. Res. **13**, 2139 (1998).

[9] C. Binns, S.H. Baker, A.M. Keen, S.N. Mozley, C. Norris, H.S. Derbyshire, and S.C. Bayliss, Phys. Rev. B **53**, 7451 (1996); M. Bumer, J. Libuda, and H.-J. Freund, Surf. Sci. **327**, 321 (1995).

[10] D.M. Duffy and J.A. Blackman, Phys. Rev. B **58**, 7443 (1998); P. Krüger, M. Taguchi, J.C. Parlebas, and A. Kotani, *ibid.* **59**, 15 093 (1999); P. Krüger, A. Rakotomahevitra, J.C. Parlebas, and C. Demangeat, *ibid.* **57**, 5276 (1998); S.S. Peng, B.R. Cooper, and Y.G. Hao, Philos. Mag. B **73**, 611 (1996).

[11] J.W. Mintmire, B.I. Dunlap, and C.T. White, Phys. Rev. Lett. **68**, 631 (1992).

[12] P. Hohenberg and W. Kohn, Phys. Rev. **136**, 864B (1964); W. Kohn and L.J. Sham, Phys. Rev. **140**, 1133A (1965).

[13] P. Ordejón, E. Artacho, and J.M. Soler, Phys. Rev. B **53**, 10 441 (1996); D. Sánchez-Portal, E. Artacho, and J.M. Soler, Int. J. Quantum Chem. **65**, 453 (1997).

[14] O.F. Sankey and D.J. Niklewski, Phys. Rev. B **40**, 3979 (1989).

[15] E. Artacho, D. Sánchez-Portal, P. Ordejón, A. Garcia, and J.M. Soler, Phys. Status Solidi B **215**, 809 (1999).

[16] J.P. Perdew, K. Burke, and M. Ernzerhof, Phys. Rev. Lett. **77**, 3865 (1996).

[17] N. Troullier and J.L. Martins, Phys. Rev. B **43**, 1993 (1991).

[18] H. Katayama-Yoshida and A. Zunger, Phys. Rev. Lett. **53**, 1256 (1984); H. Katayama-Yoshida and A. Zunger, Phys. Rev. B **31**, 7877 (1985); A. Fazzio, M. Caldas, and A. Zunger, *ibid.* **30**, 3430 (1984).

[19] The crystal-field splitting was estimated from spin-unpolarized calculations, and the exchange splitting was estimated from the center-of-gravity of the up and down *d* orbitals.

[20] R. Pandey, B.K. Rao, P. Jena, and J.M. Newsam, Chem. Phys. Lett. **321**, 142 (2000).